A Theoretical Examination of the Isomerization Pathways for $HBrO_3$ Isomers

Sujata Guha and Joseph S. Francisco*

Department of Chemistry and Department of Earth and Atmospheric Sciences, Purdue University, West Lafayette, Indiana 47907-1393

Received: April 26, 2000; In Final Form: June 30, 2000

The structures, vibrational spectra, and relative energetics of $HBrO_3$ isomers and the transition states for their isomerization have been examined using the quadratic configuration interaction method in conjunction with different basis sets. The calculated energetics for the dissociation and isomerization pathways of $HBrO_3$ show that the energy barriers for the isomerization of HOOOBr to HOOBrO (26.7 kcal mol^{-1}) and of HOOBrO to $HOBrO_2$ (22.2 kcal mol^{-1}) are large enough to prevent such isomerization from occurring. Thus, the reaction between HO_2 and BrO radicals will proceed through the exclusive formation of HOOBrO to produce HOBr and O_2. There is a possibility of the HOOOBr species being formed as well, but if this happens, HOOOBr will not isomerize to HOOBrO.

I. Introduction

The halogen that participates most effectively in catalytic cycles leading to the destruction of the ozone layer is bromine. Even though bromine compounds are less abundant in the stratosphere than chlorine compounds, it has been estimated that bromine chemistry is responsible for almost 25% of the ozone loss observed in Antarctica[1] and up to 40% of the ozone loss in the Arctic region[2] during winter. The synergistic coupling of bromine and chlorine monoxide that leads to the production of bromine and chlorine atoms greatly enhances the ozone-destroying efficiency of bromine:[3]

$$BrO + ClO \rightarrow Br + Cl + O_2 \quad (1)$$

Methyl bromide, the most abundant bromine-containing source gas used for fumigation, is primarily present in the atmosphere due to oceanic biological processes. Methyl bromide has an ozone depletion potential that exceeds the limits set by international treaties and is scheduled to be phased out in developed countries by the year 2010.[4] Most of the other important source gases containing bromine (e.g., tetrabromobisphenol A and trifluoromethyl bromide) are anthropogenic in their origin and are used as fire-retardants and refrigerants.

The catalytic cycles contributing to the destruction of ozone by bromine were initially described by Yung et al.[3] and Wofsy et al.[5] Wofsy et al. proposed the following cycle:

$$Br + O_3 \rightarrow BrO + O_2 \quad (2)$$

$$BrO + O \rightarrow Br + O_2 \quad (3)$$

$$\text{net:} \quad O + O_3 \rightarrow 2O_2 \quad (4)$$

This cycle has its greatest impact on ozone depletion in the middle and upper stratosphere. There are other catalytic cycles that occur in the lower stratosphere that couple bromine with odd hydrogen radical families. Of particular importance is the coupling of bromine oxide radicals with HO_x species (such as OH and HO_2 radicals) to destroy ozone. A critical reaction that couples BrO_x and HO_x radicals in the gas-phase catalytic cycle of bromine is the reaction between BrO and HO_2:

$$Br + O_3 \rightarrow BrO + O_2$$

$$BrO + HO_2 \rightarrow HOBr + O_2 \quad (5)$$

$$HOBr + h\nu \rightarrow OH + Br \quad (6)$$

$$OH + O_3 \rightarrow HO_2 + O_2 \quad (7)$$

$$\text{net:} \quad 2O_3 \rightarrow 3O_2 \quad (8)$$

Experimental results have suggested that reaction 5 proceeds at a substantially faster rate than that indicated by previous measurements, and may play a major role in the ozone-related chemistry of bromine compounds.

The reaction between BrO and HO_2 radicals has two thermodynamically feasible channels

$$BrO + HO_2 \rightarrow HOBr + O_2 \qquad \Delta H^\circ_{r,298} = -45.1 \text{ kcal mol}^{-1} \quad (5a)$$

$$\rightarrow HBr + O_3 \qquad \Delta H^\circ_{r,298} = -7.7 \text{ kcal mol}^{-1} \quad (5b)$$

The first study of this reaction was performed by Cox and Sheppard[6] using the molecular-modulation UV absorption technique. BrO and HO_2 were produced by photolysis of O_3 in the presence of Br_2, H_2, and O_2 and analyzed directly by UV absorption. The rate constant for the BrO + HO_2 reaction was determined as 5×10^{-12} cm^3 $molecule^{-1}$ s^{-1} at a temperature of 303 K and total pressure of 760 Torr. A similar value of the rate constant was suggested by Baulch et al.[7] for use in atmospheric modeling. Poulet et al.[8] performed a more direct study of the BrO + HO_2 reaction by means of the discharge-flow−mass-spectrometric method, determined a much higher value of the rate constant than that obtained by Cox and Sheppard, and observed HOBr to be the only product at 298 K. The higher rate constant value determined by Poulet and co-workers has been confirmed with the flash photolysis and UV absorption studies of Br_2, O_3, Cl_2, CH_3OH, O_2, and He mixtures carried out by Hayman et al.[9] and Bridier at al.[10] at 298 K and 760 Torr. The fair agreement between the three determinations suggested a value of around $k_5 = 3 \times 10^{-11}$ cm^3 $molecule^{-1}$

10.1021/jp001604s CCC: $19.00
Published on Web 09/20/2000

s^{-1} at 298 K for the BrO + HO_2 reaction. Larichev et al.[11] used discharge flow−mass spectrometry to investigate the kinetics and mechanism of the reaction between BrO and HO_2 radicals in the temperature range of 233−344 K and observed HOBr to be the major product. They obtained a rate constant value of $(4.77 \pm 0.32) \times 10^{-12}$ cm^3 $molecule^{-1}$ s^{-1} and a negative temperature dependence, suggesting the presence of an $HBrO_3$ complex. Elrod et al.[12] conducted experiments which reported a much smaller rate constant value, $(1.4 \pm 0.3) \times 10^{-11}$ cm^3 $molecule^{-1}$ s^{-1}, at 298 K. Cronkhite et al.[13] conducted laser flash photolysis studies of Cl_2, CH_3OH, O_2, Br_2, O_3, and N_2 mixtures and determined the rate constant of the BrO + HO_2 → HOBr + O_2 reaction to be $(2.0 \pm 0.6) \times 10^{-11}$ cm^3 $molecule^{-1}$ s^{-1} at 296 K. Their observations support the lower value of k_5 reported by Elrod et al. over the higher values of the rate constant obtained by Poulet et al., Bridier et al., and Larichev et al.

Mellouki and co-workers[14] tried to measure the yield of the HBr-forming channel from the BrO + HO_2 reaction and determined an upper limit on the yield of HBr by measuring an upper limit for the rate coefficient of the reverse reaction, HBr + O_3 → HO_2 + BrO. The limits measured at 300 and 441 K were extrapolated to low temperatures, and the yield of HBr was determined to be negligible (<0.01%) throughout the stratosphere. Mellouki and co-workers also observed a negative temperature dependence for the BrO + HO_2 reaction, suggesting the presence of an $HBrO_3$ complex. Garcia and Solomon[15] reported a theoretical analysis of the BrO atmospheric measurements database using a two-dimensional photochemical model and concluded that the BrO + HO_2 reaction could not have a significant yield of HBr. Li et al.[16] performed experimental studies on the BrO + HO_2 reaction over the temperature range of 233−348 K using discharge flow−mass spectrometry and found channel 5a, leading to the formation of HOBr and O_2, to be an important reaction channel. They determined the rate coefficient for the reaction of BrO and HO_2 radicals to be $(1.73 \pm 0.6) \times 10^{-11}$ cm^3 $molecule^{-1}$ s^{-1} at 298 K with excess HO_2 and $(2.05 \pm 0.64) \times 10^{-11}$ cm^3 $molecule^{-1}$ s^{-1} with excess BrO. Their overall results provided an expression for k_5 as $(3.13 \pm 0.33) \times 10^{-12}$ $\exp(536 \pm 206/T)$.

Guha and Francisco[17] examined the possibility of the formation of $HBrO_3$ complexes from the BrO + HO_2 reaction, following the suggestions of Larichev et al.[11] and Mellouki et al.[14] The order of energy levels among the $HBrO_3$ isomers that could be formed during the BrO + HO_2 reaction has been found to be $HOBrO_2$ < HOOOBr < HOOBrO < $HBrO_3$,[17] with all isomers except $HBrO_3$ lying at a lower energy level than the reactants (BrO + HO_2). Guha and Francisco[18] also examined the reaction pathways for the formation of the various complexes during the BrO + HO_2 reaction, and found that the most energetically favored pathway is the formation of HOOBrO as an intermediate and its eventual dissociation into HOBr and O_2 due to the very low energy barrier (2.8 kcal mol^{-1}) for the process.

In this paper, we present computational results of the structures, vibrational spectra, and relative energetics of the transition states of $HBrO_3$ isomers at different levels of theory to determine whether a significant energy barrier exists for the interconversion among the different isomeric forms. Knowledge of the energy barriers is very important to obtaining a complete picture of the pathways associated with the reaction between BrO and HO_2 radicals and assessing the final products of the reaction.

II. Computational Methods

Ab initio molecular orbital calculations were performed using the GAUSSIAN 94 program.[19] The equilibrium geometrical parameters of the $HBrO_3$ isomers and the transition states for their isomerization were fully optimized to better than 0.001 Å for bond distances and 0.1° for bond angles, with a self-consistent field convergence of at least 10^{-9} on the density matrix. The QCISD (quadratic configuration interaction with single and double excitations) method[20] was used with the 6-31G(d,p) and 6-311G(d,p) basis sets in the optimization of the equilibrium and transition-state structures. A second set of polarization functions supplemented the 6-311G(d,p) basis set to comprise the 6-311G(2d,2p) basis set, with which optimizations were also performed. The harmonic vibrational frequencies and infrared intensities of all species were calculated at the QCISD level of theory in conjunction with the 6-31G(d,p) basis set using the geometrical parameters calculated at the QCISD/6-31G(d,p) level of theory. To improve the energies of the species, we performed single-point calculations with the QCISD-(T) (incorporating the perturbative corrections for triple excitation) wave functions using the optimized geometrical parameters obtained at the highest level of theory [QCISD/6-311G-(2d,2p)].

III. Results and Discussion

A. Geometries and Vibrational Frequencies. Computations on the HOOOBr, HOOBrO, $HOBrO_2$, and $HBrO_3$ isomeric forms and on their isomerization transition states were performed using the QCISD method in conjunction with the 6-31G(d,p), 6-311G(d,p), and 6-311G(2d,2p) basis sets. In general, the structures optimized using the highest basis set [6-311G(2d,2p)] were found to be in good agreement with those computed using the other two basis sets. The calculated structures of the $HBrO_3$ isomeric forms agreed well with our former optimizations of the same structures at the CCSD(T)/TZ2P level of theory.[17] The structural parameters for the $HBrO_3$ isomers and their transition states are provided in parts a and b, respectively, of Table 1.

The first transition state is that for the isomerization of HOOOBr to HOOBrO, depicted in Figure 1a. This transition state is formed due to the migration of the bromine atom in HOOOBr, leading to the formation of the [HOOOBr → HOOBrO]‡ structure. Due to bromine migration, there are several structural changes observed when a comparison is made of the [HOOOBr → HOOBrO]‡ structure and the structure of the stable HOOOBr species. The O′−Br bond distance changes from 1.884 Å in HOOO′Br at the QCISD/6-311G(2d,2p) level of theory to 1.712 Å in the HOOO′Br → HOOBrO′ transition state. The O−O bond in [HOOO′Br → HOOBrO′]‡ (1.348 Å) is shorter than the corresponding O−O bond in HOOO′Br (1.422 Å). The H−O bond distances in the HOOO′Br and [HOOO′Br → HOOBrO′]‡ species are quite similar. Changes are also observed in the bond angles between the two structural forms. The HOO angle in HOOO′Br is 101.2°, while that in the HOOO′Br → HOOBrO′ transition state is slightly wider (103.7°). The OO′Br angle decreases from 110.0° in HOOO′Br to 71.0° in the [HOOO′Br → HOOBrO′]‡ structure.

Figure 1b shows the structure of the HOOBrO → $HOBrO_2$ transition state formed as a result of bromine migration in the HOOBrO species. Due to this process, certain structural differences exist between HOOBrO and the HOOBrO → $HOBrO_2$ transition state. The O−Br and Br−O′ bond distances in HOOBrO′ (1.883 and 1.674 Å, respectively) are larger than the corresponding distances in the [HOOBrO′ → $HOBrO_2$]‡

TABLE 1: Optimized Geometries (Å and deg) for $HBrO_3$ Isomers and Transition States

species	coordinates	levels of theory: QCISD/ 6-31G(d,p)	6-311G(d,p)	6-311G(2d,2p)
		(a) $HBrO_3$ Isomers		
HOOO′Br	*r*(OO′)	1.409	1.383	1.401
	r(O′Br)	1.911	1.915	1.884
	r(OO)	1.436	1.417	1.422
	r(HO)	0.972	0.966	0.963
	∠(OO′Br)	109.7	110.9	110.0
	∠(OOO′)	107.3	108.1	107.5
	∠(HOO)	101.0	101.4	101.2
	∠(OOO′Br)	79.5	82.2	80.9
	∠(HOOO′)	75.3	76.3	75.9
HOOBrO′	*r*(OBr)	1.929	1.926	1.883
	r(BrO′)	1.704	1.691	1.674
	r(OO)	1.441	1.419	1.437
	r(HO)	0.970	0.964	0.962
	∠(OBrO′)	110.8	111.7	110.6
	∠(OOBr)	109.0	110.3	109.2
	∠(HOO)	100.9	101.3	100.8
	∠(OOBrO′)	77.8	80.3	79.5
	∠(HOOBr)	96.5	99.2	99.1
$HOBrO_2$	*r*(OBr)	1.855	1.843	1.821
	r(HO)	0.975	0.969	0.967
	r(BrO)	1.652	1.628	1.621
	r(BrO′)	1.644	1.622	1.612
	∠(HOBr)	102.0	103.0	102.9
	∠(OBrO)	100.3	100.8	100.3
	∠(OBrO′)	104.0	104.1	104.0
	∠(HOBrO)	−87.6	−81.9	−92.5
	∠(HOBrO′)	28.0	34.2	23.0
$HBrO_3$	*r*(HBr)	1.471	1.474	1.467
	r(BrO)	1.631	1.607	1.601
	∠(HBrO)	102.9	103.2	103.5
		(b) Transition States		
[HOOO′Br → HOOBrO′]‡	*r*(OBr)	2.327	2.361	2.339
	r(BrO′)	1.740	1.735	1.712
	r(OO)	1.360	1.334	1.348
	r(HO)	0.974	0.968	0.965
	∠(OBrO′)	65.5	66.9	65.2
	∠(OO′Br)	69.9	69.6	71.0
	∠(HOO)	103.6	104.4	103.7
	∠(OOBrO′)	180.2	179.1	179.4
	∠(HOOBr)	91.7	91.1	92.2
[HOOBrO′ → $HOBrO_2$]‡	*r*(OBr)	1.679	1.659	1.647
	r(BrO′)	1.683	1.663	1.649
	r(OO)	2.122	2.138	2.106
	r(HO)	0.979	0.973	0.970
	∠(OBrO′)	114.3	115.1	114.0
	∠(OOBr)	75.8	76.7	77.4
	∠(HOO)	147.9	147.9	145.6
	∠(OOBrO′)	−96.1	−97.4	−95.9
	∠(HOOBr)	159.2	156.2	152.9
[$HOBrO_2$ → $HBrO_3$]‡	*r*(O′Br)	1.727	1.707	1.694
	r(HBr)	1.530	1.528	1.545
	r(BrO)	1.645	1.623	1.614
	∠(HBrO′)	60.6	60.5	60.3
	∠(OBrO′)	112.2	112.1	111.7
	∠(HBrO)	121.3	121.5	122.1
	∠(OBrO)	114.9	114.6	113.9
	∠(HBrO′O)	68.1	69.4	68.5
	∠(OBrOO′)	131.1	132.5	131.9

structure (1.647 and 1.649 Å, respectively). The H−O bond length increases by 0.008 Å between HOOBrO′ and [HOOBrO′ → $HOBrO_2$]‡, and the O−O bond length increases by 0.669 Å between the two structures. The HOO angle in [HOOBrO′ → $HOBrO_2$]‡ (145.6°) is much wider than the HOO angle in HOOBrO′ (100.8°), while the OOBr angle in HOOBrO′ (109.2°) is wider than the corresponding OOBr angle in the HOOBrO′ → $HOBrO_2$ transition state. The OBrO′ angle is 3.4° narrower in HOOBrO′ compared to that in the [HOOBrO′ → $HOBrO_2$]‡ structure.

The final transition state is that for the isomerization of $HOBrO_2$ to $HBrO_3$ due to the migration of the hydrogen atom in $HOBrO_2$ (Figure 1c). A comparison of the structures of [$HOBrO_2$ → $HBrO_3$]‡ and the stable $HOBrO_2$ species shows distinct differences. The O−Br bond length decreases from 1.821 Å in $HOBrO_2$ to 1.614 Å in [$HOBrO_2$ → $HBrO_3$]‡. Due to the changes in conformation during the isomerization process, the H−Br bond present in the $HOBrO_2$ → $HBrO_3$ transition-state structure is absent in $HOBrO_2$. The OBrO′ and OBrO angles are about 8° and 14°, respectively, wider in the [$HOBrO_2$

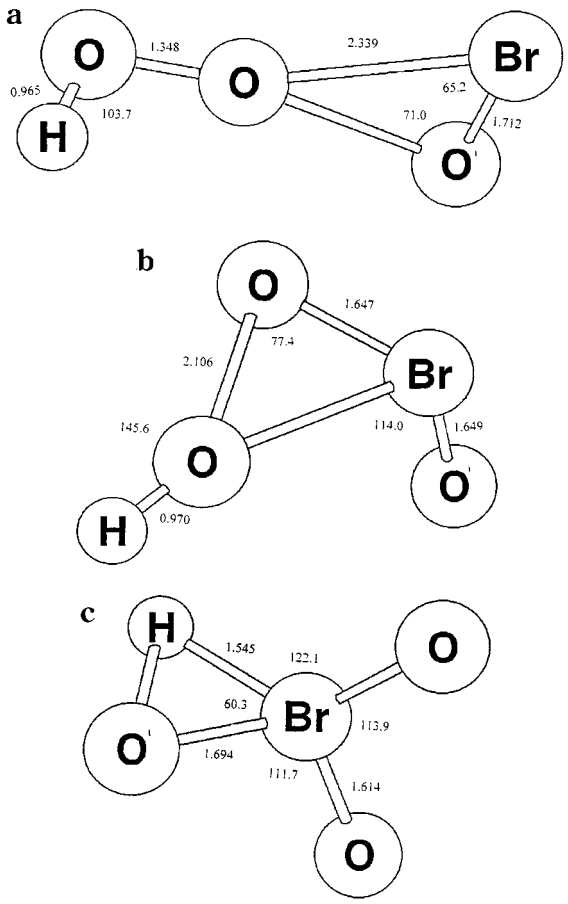

Figure 1. Transition states for $HBrO_3$ isomerization pathways: (a) HOOOBr → HOOBrO, (b) HOOBrO → $HOBrO_2$, and (c) $HOBrO_2$ → $HBrO_3$.

→ $HBrO_3]^‡$ structure compared to the those in the structure of $HOBrO_2$.

The calculated harmonic vibrational frequencies and intensities for the $HBrO_3$ isomers and their transition states are provided in parts a and b, respectively, of Table 2. The vibrational frequencies are calculated at the QCISD level of theory in conjunction with the 6-31G(d,p) basis set.

A comparison of the frequencies of HOOOBr and the [HOOOBr → HOOBrO]‡ isomerization transition state reveals certain interesting features. The [HOOO′Br → HOOBrO′]‡ structure has an imaginary frequency, the characteristic of a true transition state, suggesting that it is a first-order saddle point. The H−O stretch in [HOOO′Br → HOOBrO′]‡ occurs at a slightly higher frequency and intensity than the H−O stretch in HOOO′Br. The O−O stretch in the HOOO′Br → HOOBrO′ transition state (998 cm^{-1}) is higher in frequency than the O−O stretch in HOOO′Br (928 cm^{-1}), consistent with the longer O−O bond in HOOO′Br compared to the O−O bond in the transition state. The HOO bend in the [HOOO′Br → HOOBrO′]‡ structure at 1442 cm^{-1} is comparable to the HOO bend in the HOOO′Br species. The OOO′ bend at 587 cm^{-1} in HOOO′Br is absent in the [HOOO′Br → HOOBrO′]‡ structure.

The transition state for the isomerization of HOOBrO to $HOBrO_2$ also has an imaginary frequency. The frequencies of the [HOOBrO′ → $HOBrO_2]^‡$ structure exhibit certain differences when compared to the frequencies of HOOBrO′, due to the differences between the two conformations. The Br−O symmetric and asymmetric stretches in the HOOBrO′ → $HOBrO_2$ transition state (850 and 739 cm^{-1}, respectively) are larger than the corresponding Br−O symmetric and asymmetric stretches in HOOBrO′ (801 and 476 cm^{-1}, respectively), consistent with the longer Br−O bond in HOOBrO′. The OBrO′ bend in [HOOBrO′ → $HOBrO_2]^‡$ occurs at a higher frequency (331 cm^{-1}) and intensity (74 km mol^{-1}) than the OBrO′ bend in HOOBrO′. The H−O and O−O stretches in HOOBrO′ occur at higher frequencies than the corresponding H−O and O−O stretches in the HOOBrO′ → $HOBrO_2$ transition state, consistent with the longer H−O and O−O bonds in the [HOOBrO′ → $HOBrO_2]^‡$ structure.

The final transition-state structure is that for the isomerization of $HOBrO_2$ to $HBrO_3$, which also has an imaginary frequency. The frequencies of the [$HOBrO_2$ → $HBrO_3]^‡$ conformation differ to some extent from those of $HOBrO_2$. The Br−O symmetric stretch in the $HOBrO_2$ → $HBrO_3$ transition state (904 cm^{-1}) occurs at a higher frequency, while the Br−O asymmetric stretch (866 cm^{-1}) occurs at a lower frequency, than the corresponding Br−O stretches in the $HOBrO_2$ structure. The H−Br stretch present in [$HOBrO_2$ → $HBrO_3]^‡$ is absent in $HOBrO_2$ due to differences in structures between the two species. The HOBr bending mode that appears at 1136 cm^{-1} in $HOBrO_2$ is not present in [$HOBrO_2$ → $HBrO_3]^‡$. The hydrogen-wagging mode appears at a higher frequency in the $HOBrO_2$ → $HBrO_3$ transition state than in $HOBrO_2$.

B. Relative Energetics of $HBrO_3$ Isomers and Transition States. The total energies of the $HBrO_3$ intermediates and the isomerization transition states are provided in parts a and b, respectively, of Table 3. The energies are obtained at the QCISD level of theory using the 6-31G(d,p), 6-311G(d,p), and 6-311G(2d,2p) basis sets. Table 3 also lists single-point energy data obtained from the calculations at the QCISD(T) level of theory with the 6-311G(2d,2p), 6-311++G(2d,2p), 6-311++G(2df,2p), and 6-311++G(3df,3pd) basis sets and the optimized geometrical parameters from the QCISD/6-311G(2d,2p) level of theory. Table 4 contains information about the heats of reaction and heights of the energy barriers for the HOOOBr → HOOBrO, HOOBrO → $HOBrO_2$, and $HOBrO_2$ → $HBrO_3$ transition states at the QCISD and QCISD(T) levels of theory using various basis sets. Zero-point energy corrections are included in the calculation of the relative energetics for all structures (see Figure 2).

A comparison of the energy values among HOOOBr, HOOBrO, $HOBrO_2$, and $HBrO_3$, listed in Table 3a, shows that at the QCISD/6-31G(d,p), QCISD/6-311G(d,p), QCISD/6-311G(2d,2p), QCISD(T)/6-311G(2d,2p), and QCISD(T)/6-311++G(2d,2p) levels of theory, the order of decreasing stability among the isomers is HOOOBr > $HOBrO_2$ > HOOBrO > $HBrO_3$, with HOOOBr being the most stable structural form. This order of stability, however, becomes reversed with the addition of higher-order polarization functions beginning with the incorporation of the 6-311++G(2df,2p) basis set, and the order of increasing energies among the four isomers at the QCISD(T)/6-311++G(2df,2p) and QCISD(T)/6-311++G(3df,3pd) levels of theory appears as $HOBrO_2$ < HOOOBr < HOOBrO < $HBrO_3$, with the $HOBrO_2$ structure possessing the least energy. This indicates that with the addition of diffuse and *f* polarization functions, $HOBrO_2$ becomes more stable than HOOOBr. The observation of $HOBrO_2$ being the most stable isomeric form is consistent with our earlier prediction[17] of the relative energetic stability among the $HBrO_3$ isomers. There appears to be very good agreement between the total and single-point energies for the $HBrO_3$ isomers due to the good convergence of the numerical values. The order of increasing energies among the transition states, as presented in Table 3b, is [HOOOBr → $HOOBrO]^‡$ < [HOOBrO → $HOOBrO_2]^‡$ < [$HOBrO_2$ →

TABLE 2: Harmonic Frequencies (cm^{-1}) and IR Intensities (km mol^{-1}) for $HBrO_3$ Isomers and Transition States

			QCISD/6-31G(d,p)	
species	mode numbers	mode description	frequencies	intensities
		(a) $HBrO_3$ Isomers		
HOOO′Br	1	HO stretch	3726	40
	2	HOO bend	1435	48
	3	OO stretch	928	31
	4	OO′ stretch	851	24
	5	OOO′ bend	587	6
	6	BrO′ stretch	517	25
	7	HOOO′ torsion	437	91
	8	BrO′O bend	295	11
	9	BrO′OO torsion	131	4
HOOBrO′	1	HO stretch	3734	43
	2	HOO bend	1441	49
	3	OO stretch	962	58
	4	BrO sym. str.	801	25
	5	BrO asym. str.	476	74
	6	H-wag	444	34
	7	BrOO bend	268	1
	8	OBrO′ bend	192	10
	9	torsion	38	3
$HOBrO_2$	1	HO stretch	3747	85
	2	HOBr bend	1136	46
	3	BrO asym. str.	925	81
	4	BrO sym. str.	848	26
	5	BrO′ stretch	525	78
	6	OBrO bend	360	39
	7	OBrO′ bend	333	60
	8	OBrO′ bend	285	26
	9	H-wag	193	38
$HBrO_3$	1	HBr stretch	2205	54
	2	BrO sym. str.	821	13
	3	umbrella	380	44
	4	BrO asym. str.	953′	85
	5	HBrO bend	925′	0
	6	OBrO bend	331′	21
		(b) Transition States		
[HOOO′Br → HOOBrO′]‡	1	HO stretch	3733	72
	2	HOO bend	1442	27
	3	OO stretch	998	394
	4	BrO′ stretch	708	110
	5	OBr stretch	530	128
	6	OBrO′ bend	439	15
	7	OO′Br bend	239	6
	8	H-wag	150	9
	9	reaction coord.	175i	9
[HOOBrO′ → $HOBrO_2$]‡	1	HO stretch	3702	60
	2	BrO sym. str.	850	10
	3	HOO bend	796	105
	4	BrO asym. str.	739	34
	5	OO stretch	352	48
	6	OBrO′ bend	331	74
	7	OOBr bend	307	28
	8	HOOBr torsion	142	11
	9	reaction coord.	632i	108
[$HOBrO_2$ → $HBrO_3$]‡	1	HBr stretch	1969	13
	2	BrO sym. str.	904	65
	3	BrO asym. str.	866	81
	4	O′Br stretch	749	14
	5	H-wag	521	2
	6	OBrO bend	334	29
	7	OBrOO′ torsion	297	14
	8	HBrO′O torsion	285	15
	9	reaction coord.	1414i	288

$HBrO_3$]‡ at all levels of theory, indicating that the isomerization of HOOOBr to HOOBrO requires the least energy.

From Table 4, it is observed that the HOOOBr → HOOBrO transition state possesses a heat of reaction of 13.7 kcal mol^{-1} and an energy barrier of 26.7 kcal mol^{-1} at 0 K. For the HOOBrO → $HOBrO_2$ isomerization, the heat of reaction is −20.7 kcal mol^{-1}, and the energy barrier is 22.2 kcal mol^{-1}. Thus, there appears to be a lower energy barrier (by ∼5 kcal mol^{-1}) for the isomerization of HOOBrO to $HOBrO_2$ relative to the HOOOBr → HOOBrO isomerization. The values for the heat of reaction and energy barrier for the $HOBrO_2$ → $HBrO_3$ transition state are 65.6 and 89.4 kcal mol^{-1}, respectively. The process of isomerization of $HOBrO_2$ to $HBrO_3$, therefore, possesses significantly higher energy barriers relative to the HOOOBr → HOOBrO isomerization (by ∼63 kcal mol^{-1}) and the HOOBrO → $HOBrO_2$ isomerization (by ∼67 kcal mol^{-1}). From Table 4, it is apparent that the HOOBrO → $HOBrO_2$ transition state has the lowest energy barrier height (relative to

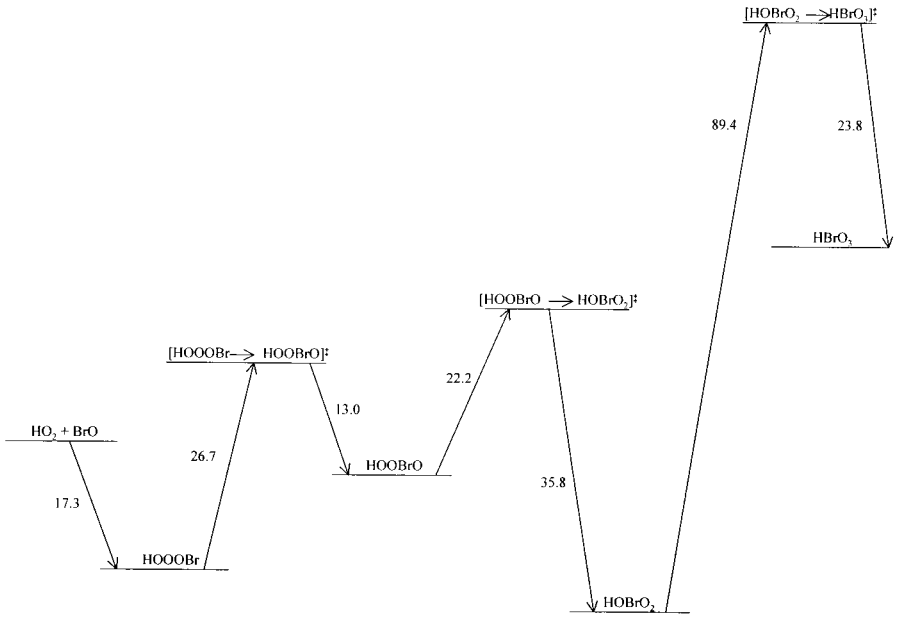

Figure 2. Energetics of the $HBrO_3$ isomerization pathways.

TABLE 3: Total and Single-Point Energies (hartrees) for $HBrO_3$ Isomers and Transition States

(a) $HBrO_3$ Isomers

levels of theory	HOOOBr	HOOBrO	$HOBrO_2$	$HBrO_3$
QCISD/6-31G(d,p)	−2795.48803	−2795.44681	−2795.45641	−2795.34157
QCISD/6-311G(d,p)	−2798.08546	−2798.03816	−2798.04755	−2797.93483
QCISD/6-311G(2d,2p)	−2798.14551	−2798.10178	−2798.12963	−2798.01982
QCISD(T)/6-311G(2d,2p)[a]	−2798.17910	−2798.14576	−2798.16750	−2798.05796
QCISD(T)/6-311++G(2d,2p)[a]	−2798.19169	−2798.16316	−2798.18362	−2798.07214
QCISD(T)/6-311++G(2df,2p)[a]	−2798.29391	−2798.26951	−2798.30021	−2798.19258
QCISD(T)/6-311++G(3df,3pd)[a]	−2798.32066	−2798.29758	−2798.33054	−2798.22475

(b) Transition States

levels of theory	$[HOOOBr \rightarrow HOOBrO]^{\ddagger}$	$[HOOBrO \rightarrow HOBrO_2]^{\ddagger}$	$[HOBrO_2 \rightarrow HBrO_3]^{\ddagger}$
QCISD/6-31G(d,p)	−2795.41720	−2795.37855	−2795.29573
QCISD/6-311G(d,p)	−2798.01159	−2797.96978	−2797.88634
QCISD/6-311G(2d,2p)	−2798.07526	−2798.04372	−2797.97060
QCISD(T)/6-311G(2d,2p)[a]	−2798.13127	−2798.10239	−2798.01586
QCISD(T)/6-311++G(2d,2p)[a]	−2798.14792	−2798.12346	−2798.03190
QCISD(T)/6-311++G(2df,2p)[a]	−2798.24897	−2798.23011	−2798.15025
QCISD(T)/6-311++G(3df,3pd)[a]	−2798.27651	−2798.25970	−2798.18242

[a] Calculated using the QCISD/6-311G(2d,2p) geometrical parameters.

TABLE 4: Relative Energetics (kcal mol^{-1}) for $HBrO_3$ Isomerization Transition States

	$[HOOOBr \rightarrow HOOBrO]^{\ddagger}$		$[HOOBrO \rightarrow HOBrO_2]^{\ddagger}$		$[HOBrO_2 \rightarrow HBrO_3]^{\ddagger}$	
levels of theory	$\Delta H_{r,0}^{\circ}$	barrier heights	$\Delta H_{r,0}^{\circ}$	barrier heights	$\Delta H_{r,0}^{\circ}$	barrier heights
QCISD/6-31G(d,p)	25.1	43.4	−6.0	41.2	71.3	97.3
QCISD/6-311G(d,p)	28.9	45.4	−5.9	41.3	69.9	97.7
QCISD/6-311G(2d,2p)	26.6	43.1	−17.5	34.8	68.1	96.3
QCISD(T)/6-311G(2d,2p)	20.1	29.0	−13.6	25.6	67.9	91.7
QCISD(T)/6-311++G(2d,2p)	17.1	26.5	−12.8	23.3	69.2	91.7
QCISD(T)/6-311++G(2df,2p)	14.5	27.2	−19.3	23.1	66.7	90.6
QCISD(T)/6-311++G(3df,3pd)	13.7	26.7	−20.7	22.2	65.6	89.4

the $HOOOBr \rightarrow HOOBrO$ and $HOBrO_2 \rightarrow HBrO_3$ transition states), and thus, that transition state is the most stabilized.

From the overall results of our study, it is observed that the reaction between BrO and HO_2 radicals may proceed through the formation of either the HOOOBr or the HOOBrO intermediate to produce the final products (HOBr and O_2). Our previous calculations[18] suggest that the most likely pathway during the $BrO + HO_2$ reaction is the formation of HOOBrO as a complex intermediate and its eventual dissociation into HOBr and O_2, since the process has a very low energy barrier (2.8 kcal mol^{-1}). As shown by our present calculations, it is very unlikely that the HOOBrO intermediate would isomerize to HOOOBr or $HOBrO_2$ due to the high energy barriers associated with the processes (26.7 and 22.2 kcal mol^{-1}, respectively). If HOOOBr is formed as an intermediate, it will not isomerize to HOOBrO.

IV. Conclusion

The equilibrium structures, vibrational spectra, and relative energetics of the possible $HBrO_3$ isomers formed during the $BrO + HO_2$ reaction and the $HOOOBr \rightarrow HOOBrO$, HOOBrO

→ $HOBrO_2$, and $HOBrO_2$ → $HBrO_3$ isomerization transition states have been investigated with different ab initio methods. The HOOBrO (or HOOOBr) species can be formed as intermediates during the reaction of BrO radicals with HO_2, but it is not possible for them to interconvert due to the presence of a large energy barrier for the isomerization process.

References and Notes

(1) Anderson, J. G.; Toohey, D. W.; Brune, W. H. *Science* **1991**, *251*, 39.

(2) Salawitch, R. J.; McElroy, M. B.; Yatteau, J. H.; Wofsy, S. C.; Schoeberl, M. R.; Lait, L. R.; Newman, P. A.; Chan, K. R.; Loewenstein, M.; Podolske, J. R.; Strahan, S. E.; Proffitt, M. H. *Geophys. Res. Lett.* **1990**, *17*, 561.

(3) Yung, Y. L.; Pinto, J. P.; Watson, R. T.; Sander, S. P. *J. Atmos. Sci.* **1980**, *37*, 339.

(4) World Meteorological Organization. *Scientific Assessment of Ozone Depletion*; National Aeronautics and Space Administration: Houston, TX, 1994.

(5) Wofsy, S. C.; McElroy, M. D.; Yung, Y. L. *Geophys. Res. Lett.* **1975**, *2*, 215.

(6) Cox, R. A.; Sheppard, D. W. *J. Chem. Soc., Faraday Trans., 2* **1982**, *78*, 1383.

(7) Baulch, D. L.; Cox, R. A.; Hampton, R. F., Jr.; Kerr, J. A.; Troe, J.; Watson, R. T. *J. Phys. Chem. Ref. Data* **1980**, *9*, 295.

(8) Poulet, G.; Pirre, M.; Maguin, F.; Ramaroson, R.; Le Bras, G. *Geophys. Res. Lett.* **1992**, *19*, 2305.

(9) Hayman, G. D.; Danis, F.; Thomas, D. H. J.; Peeters, R. A. *Air Pollution*; Report45; Commission of the European Communities: Brussels, Belgium, 1993.

(10) Bridier, I.; Veyret, B.; Lesclaux, R. *Chem. Phys. Lett.* **1993**, *201*, 563.

(11) Larichev, M.; Maguin, F.; Le Bras, G.; Poulet, G. *J. Phys. Chem.* **1995**, *99*, 15911.

(12) Elrod, M. J.; Meads, R. F.; Lipson, J. B.; Seeley, J. V.; Molina, M. J. *J. Phys. Chem.* **1996**, *100*, 5808.

(13) Cronkhite, J. M.; Stickel, R. E.; Nicovich, J. M.; Wine, P. H. *J. Phys. Chem. A* **1998**, *102*, 6651.

(14) Mellouki, A.; Talukdar, R. K.; Howard, C. J. *J. Geophys. Res.* **1994**, *99*, 22949.

(15) Garcia, R. R.; Solomon, S. *J. Geophys. Res.* **1994**, *99*, 12937.

(16) Li, Z.; Friedl, R. R.; Sander, S. P. *J. Chem. Soc., Faraday Trans.* **1997**, *93*, 2683.

(17) Guha, S.; Francisco, J. S. *J. Phys. Chem. A* **1998**, *102*, 2072.

(18) Guha, S.; Francisco, J. S. *J. Phys. Chem. A* **1999**, *103*, 8000.

(19) Frisch, M. J.; Trucks, G. W.; Schlegel, H. B.; Gill, P. M. W.; Johnson, B. G.; Robb, M. A.; Cheeseman, J. R.; Keith, T.; Petersson, G. A.; Montgomery, J. A.; Raghavachari, K.; Al-Laham, M. A.; Zakrzewski, V. G.; Ortiz, J. V.; Foresman, J. B.; Cioslowski, J.; Stefanov, B. B.; Nanayakkara, A.; Challacombe, M.; Peng, C. Y.; Ayala, P. Y.; Chen, W.; Wong, M. W.; Andres, J. L.; Replogle, E. S.; Gomperts, R.; Martin, R. L.; Fox, D. J.; Binkley, J. S.; Defrees, D. J.; Baker, J.; Stewart, J. P.; Head-Gordon, M.; Gonzales, C.; Pople, J. A. *GAUSSIAN 94*, Revision D.2; Gaussian: Pittsburgh, PA, 1995.

(20) Pople, J. A.; Head-Gordon, M.; Raghavachari, K. *J. Chem. Phys.* **1987**, *87*, 5968.